Inorganic Chemistry
Article

Inorg. Chem. **2010**, *49*, 6453–6460 **6453**
DOI: 10.1021/ic100036v

A Highly Stable Rhenium−Cobalt System for Photocatalytic H_2 Production: Unraveling the Performance-Limiting Steps

Benjamin Probst,[†] Alexander Rodenberg,[‡] Miguel Guttentag,[†] Peter Hamm,*[,‡] and Roger Alberto*[,†]

[†]*Institute of Inorganic Chemistry,* [‡]*Institute of Physical Chemistry, University of Zürich, Winterthurerstrasse 190, CH-8057 Zürich Switzerland*

Received January 7, 2010

Increased long-term performance was found for photocatalytic H_2 production in a homogeneous combination of [Re(NCS)(CO)$_3$bipy] (**1**; bipy = 2,2′-bipyridine), [Co(dmgH)$_2$] (dmgH$_2$ = dimethylglyoxime), triethanolamine (TEOA), and [HTEOA][BF_4] in *N,N*-dimethylformamide, achieving TON_{Re} up to 6000 (H/Re). The system proceeded by reductive quenching of ***1** by TEOA, followed by fast ($k_1 = 1.3 \times 10^8$ M^{-1} s^{-1}) electron transfer to [Co^{II}(dmgH)$_2$] and subsequent protonation (K_2) and elimination (k_3, second-order process in cobalt) of H_2. Observed quantum yields were up to ∼90% (H produced per absorbed photon). The type of acid had a substantial effect on the long-term stability. A decomposition pathway involving cobalt is limiting the long-term performance. Time-resolved infrared (IR) spectroscopy confirmed that photooxidized TEOA generates a second reducing equivalent, which can be transferred to **1** (70%, $k_{2e^-} = 3.3 \times 10^8$ M^{-1} s^{-1}) if no [Co^{II}(dmgH)$_2$] is present.

Introduction

The long-term objective of this study is to find a photocatalytic cycle in a homogeneous solution for water splitting to H_2 and O_2 and is motivated by ongoing depletion of fossil energy sources in the years to come. Commercially available photovoltaic (PV) cells coupled to state-of-the-art water electrolyzers split water in high yields, but at prices that do not yet compete with H_2 produced by steam reforming of natural gas or coal gasification.[1] This intrinsic problem will, however, be overcome as soon as prices for fossil fuels rise significantly. Besides PV cells, the search for direct light-driven processes represents an incentive in current research. A particularly appealing one is the mimicking of natural photosynthesis: photons are absorbed by a photosensitizer to generate free electrons and holes. Ideally, the latter ones can be used for water oxidation, while the electrons reduce water (Scheme 1).

First literature reports about photocatalytic water splitting in homogeneous solutions appeared around 1980 with the pioneering work of Sutin and Lehn.[2,3] They presented systems that reduced protons to H_2 with $[Ru(bipy)_3]^{2+}$ as a photosensitizer (PS) and a cobalt-based water reduction catalyst (WRC). Cobalt macrocyclic complexes acted as WRCs in some more recent reports about photocatalytic proton reduction. Artero et al. applied [$Co(dmgX)_2YZ$]-type complexes (dmgH$_2$ = dimethylglyoxime, X = H^+ or BF_2^+, Y = halogen, Z = pyridine derivatives) and [$ReBr(CO)_3$phen]-, $[Ru(diimine)_3]^{2+}$-, and $[Ir(ppy)(diimine)]^+$-type PSs, with the latter two complexes also with a covalent link to the axial pyridine coordinated to cobalt, achieving up to 550 turnover numbers (TONs; for H/Re and 275 for H_2/Co) with the rhenium system.[4,5] Eisenberg et al. focused on [$Co(dmgX)_2$-YZ]-type complexes but with a platinum terpyridyl acetylide or, more recently, xanthene-type PSs, achieving up to 2400 TONs (for H/Pt and 2200 for H_2/Co) in the platinum system.[6,7] In our own work, [$ReBr(CO)_3$bipy] served as the PS and [Co(dmgH)$_2$] as the WRC.[8] Bernhard et al. used $[M(bipy)_3]^{3+}$ (M = Co^{III} or Rh^{III}) as WRC in combination with $[Ir(ppy)_2(diimine)]^+$ as the PS in MeCN or tetrahydrofuran/water mixtures with TONs up to a respectable 5000 (for H/Ir and 2500 for H_2/Rh).[9,10] Other more recent systems were all based on $[Ru(bipy)_3]^{2+}$-type PSs and platinum, palladium, or rhodium complexes as WRCs.[11−14] Besides displaying low TONs (5−50), the homogeneous character of

*To whom correspondence should be addressed. E-mail: ariel@aci.uzh.ch.

(1) Drennen, T. E.; Rosthal, J. E. *Pathways to a hydrogen future*; Elsevier: Amsterdam, The Netherlands, 2007.
(2) Brown, G. M.; Brunschwig, B. S.; Creutz, C.; Endicott, J. F.; Sutin, N. *J. Am. Chem. Soc.* **1979**, *101*, 1298–1300.
(3) Hawecker, J.; Lehn, J. M.; Ziessel, R. *New J. Chem.* **1983**, *7*, 271–277.
(4) Fihri, A.; Artero, V.; Razavet, M.; Baffert, C.; Leibl, W.; Fontecave, M. *Angew. Chem., Int. Ed.* **2008**, *47*, 564–567.
(5) Fihri, A.; Artero, V.; Pereira, A.; Fontecave, M. *Dalton Trans.* **2008**, 5567–5569.
(6) Du, P.; Schneider, J.; Luo, G.; Brennessel, W. W.; Eisenberg, R. *Inorg. Chem.* **2009**, *48*, 4952–4962.
(7) Lazarides, T.; McCormick, T.; Du, P. W.; Luo, G. G.; Lindley, B.; Eisenberg, R. *J. Am. Chem. Soc.* **2009**, *131*, 9192–.
(8) Probst, B.; Kolano, C.; Hamm, P.; Alberto, R. *Inorg. Chem.* **2009**, *48*, 1836–1843.
(9) Cline, E. D.; Adamson, S. E.; Bernhard, S. *Inorg. Chem.* **2008**, *47*, 10378–10388.
(10) Goldsmith, J. I.; Hudson, W. R.; Lowry, M. S.; Anderson, T. H.; Bernhard, S. *J. Am. Chem. Soc.* **2005**, *127*, 7502–7510.

Published on Web 06/16/2010

Scheme 1. General Representation of a Photocatalytic Relay for Water Decomposition into H_2 and O_2 Proceeding via Reductive Quenching of the Excited *PS by a WOC and Subsequent Reduction of a WRC by PS^-

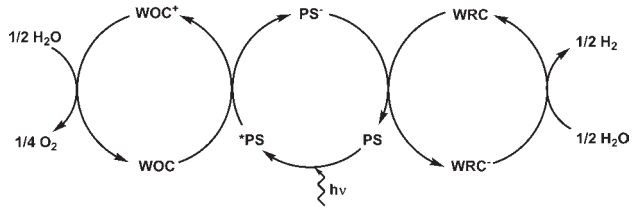

these latter systems was put into question.[12] Great efforts have been put into the development of water oxidation catalysts (WOCs),[15−20] and the first examples of photocatalytic water oxidation reactions (to our knowledge) were only recently reported by Hill et al.[21] and Sun et al.[22]

Our initial studies focused on the kinetics and short-term performance of a homogeneous system using triethanolamine (TEOA) as the sacrificial electron donor, [$ReBr(CO)_3$bipy] as the PS, and [$Co(dmgH)_2$] as the WRC. We found that reductive quenching of *PS by TEOA was followed by fast ($k_{1,Br} = 2.5 \times 10^8\ M^{-1}\ s^{-1}$) electron transfer to [$Co^{II}(dmgH)_2$]. The resulting Co^I species produced H_2 in a second-order process in cobalt. The long-term performance of the process was limited by [$ReBr(CO)_3$bipy]. The labile Br^- ligand was lost under photocatalytic conditions after a short time of irradiation, thereby interrupting the cycle. We also found that acetic acid had a negative influence on the long-term performance of the system.

Addressing these two drawbacks, we present in this report a substantially improved system. Replacing Br^- in [$ReBr(CO)_3$bipy] by $[NCS]^-$ and acetic acid by [HTEOA][BF_4] increased the long-term stability significantly (TON_{Re} up to 6000). Electron transfer between the reduced PS and Co^{II} was very fast ($k_1 = 1.3 \times 10^8\ M^{-1}\ s^{-1}$). The transfer of a second reducing equivalent to the PS, tentatively assigned to originate from decomposition of TEOA, could be observed. Potential rhenium decomposition pathways were identified in a domain where the cobalt concentration was rate-limiting. We confirmed a second-order process in cobalt for the final formation of H_2 and a strong correlation between $[HTEOA^+]$ and the initial turnover frequency (TOF) and the end TON, respectively.

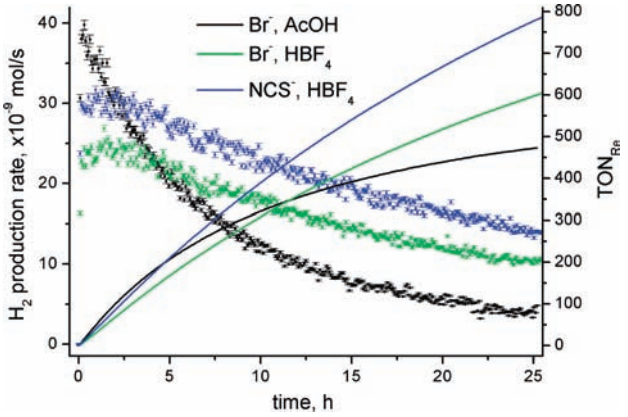

Figure 1. H_2 production rate (left scale, ■) and TON_{Re} (right scale, solid lines) as a function of time with AcOH or HBF_4, respectively, and with X = Br^- or NCS^- (0.5 mM [$ReX(CO)_3$bipy], 1 mM $[Co(OH_2)_6](BF_4)_2$, 6 mM $dmgH_2$, 1 M TEOA, 0.1 M acid, DMF, Ar, 476 nm).

Results and Discussion

Influence of Acid and X in [$ReX(CO)_3$bipy] on H_2 Production. Analysis of the reaction mixtures in the TEOA/AcOH/[$ReBr(CO)_3$bipy]/[$Co(dmgH)_2$]/DMF system after irradiation revealed the quantitative loss of Br^- in [$ReBr(CO)_3$bipy]. The addition of a 10-fold excess of tetra-*n*-butylammonium bromide ([TBA]Br) did not increase the catalytic performance (see SI 1 in the Supporting Information). Replacing acetic acid ($pK_a = 13-14$)[23] by [HTEOA][BF_4] ($pK_a = 7.5$)[23] considerably increased the long-term performance, although at lower rates (see Figure 1). The axial bromide ligand now remained coordinated to rhenium, as evidenced by high-performance liquid chromatography (HPLC). Obviously, acetic acid accelerates the loss of Br^- from [$ReBr(CO)_3$bipy], possibly via formation of an acetate or a solvato complex. Accordingly, comparative experiments were performed with [$Re(OH_2)(CO)_3$bipy][O_3SCF_3], where axial-bound OH_2 served as a leaving group. Indeed, we found catalysis to proceed at a much lower, albeit a constant rate, as found for [$ReBr(CO)_3$bipy] after the initial burst in H_2 production (see SI 1 in the Supporting Information). This confirmed our hypothesis that loss of axial Br^- in [$ReBr(CO)_3$bipy] limited H_2 production in the previous system. We hypothesized that the lower TOF for $[Re(OH_2)(CO)_3bipy]^+$ is due to a reduced overlap with the 476 nm LED (Table 1 and SI 7 in the Supporting Information). This assumption was supported by experiments with a 380 nm LED (see SI 5 in the Supporting Information), where extinction of $[Re(OH_2)(CO)_3bipy]^+$ and [$ReBr(CO)_3$bipy] and H_2 production were almost equal.

To further evidence the influence of the axial ligand X^-, we replaced [$ReBr(CO)_3$bipy] by [$Re(NCS)(CO)_3$bipy] (**1**). We found previously that **1** exerts a very high stability[24] while maintaining physicochemical properties

(11) Elvington, M.; Brown, J.; Arachchige, S. M.; Brewer, K. J. *J. Am. Chem. Soc.* **2007**, *129*, 10644–.
(12) Lei, P.; Hedlund, M.; Lomoth, R.; Rensmo, H.; Johansson, O.; Hammarstrom, L. *J. Am. Chem. Soc.* **2008**, *130*, 26–27.
(13) Ozawa, H.; Haga, M. A.; Sakai, K. *J. Am. Chem. Soc.* **2006**, *128*, 4926–4927.
(14) Rau, S.; Schafer, B.; Gleich, D.; Anders, E.; Rudolph, M.; Friedrich, M.; Gorls, H.; Henry, W.; Vos, J. G. *Angew. Chem., Int. Ed.* **2006**, *45*, 6215–6218.
(15) Chen, H. Y.; Tagore, R.; Das, S.; Incarvito, C.; Faller, J. W.; Crabtree, R. H.; Brudvig, G. W. *Inorg. Chem.* **2005**, *44*, 7661–7670.
(16) Geletii, Y. V.; Botar, B.; Koegerler, P.; Hillesheim, D. A.; Musaev, D. G.; Hill, C. L. *Angew. Chem., Int. Ed.* **2008**, *47*, 3896–3899.
(17) Gersten, S. W.; Samuels, G. J.; Meyer, T. J. *J. Am. Chem. Soc.* **1982**, *104*, 4029–4030.
(18) McDaniel, N. D.; Coughlin, F. J.; Tinker, L. L.; Bernhard, S. *J. Am. Chem. Soc.* **2008**, *130*, 210–217.
(19) Sartorel, A.; Carraro, M.; Scorrano, G.; De Zorzi, R.; Geremia, S.; McDaniel, N. D.; Bernhard, S.; Bonchio, M. *J. Am. Chem. Soc.* **2008**, *130*, 5006–5007.
(20) Tseng, H. W.; Zong, R.; Muckerman, J. T.; Thummel, R. *Inorg. Chem.* **2008**, *47*, 11763–11773.
(21) Geletii, Y. V.; Huang, Z.; Hou, Y.; Musaev, D. G.; Lian, T.; Hill, C. L. *J. Am. Chem. Soc.* **2009**, *131*, 7522–7523.
(22) Duan, L.; Xu, Y.; Zhang, P.; Wang, M.; Sun, L. *Inorg. Chem.* **2009**, *49*, 209–215.
(23) Izutsu, K. *Acid−base dissociation constants in dipolar aprotic solvents*; Blackwell Scientific Publications: Oxford, U.K., 1990.
(24) Kurz, P.; Probst, B.; Spingler, B.; Alberto, R. *Eur. J. Inorg. Chem.* **2006**, 2966–2974.

Table 1. Physicochemical Properties of $[ReX(CO)_3bipy]$ in DMF

X	λ_{MLCT}, nm (ε, $M^{-1}\,s^{-1}$)	λ_{phos}, nm ($\Phi \times 10^3$)	τ, ns	$k_{q,TEOA}$, $\times 10^6\ M^{-1}\,s^{-1}$	E_{red},[a] V	$\nu_{CO,\,sym}$,[b] cm^{-1}
Br	375 (3110 ± 50)	600 (1.8 ± 0.11)	42.2 ± 0.19	64.8 ± 0.4	−1.235	2011
OH_2	347 (sh; 3950 ± 20)	590 (1.5 ± 0.07)	33.3 ± 0.16	236 ± 3.2	−1.080	2035
NCS	376 (2910 ± 99)	602 (1.1 ± 0.05)	25.5 ± 0.22	92 ± 1.2	−1.185	2020

[a] Reversible one-electron reduction potentials in V vs Ag/AgCl. [b] In KBr pellet.

Scheme 2. Sequence of Reactions (As Assumed) for TEOA upon Interaction with *PS

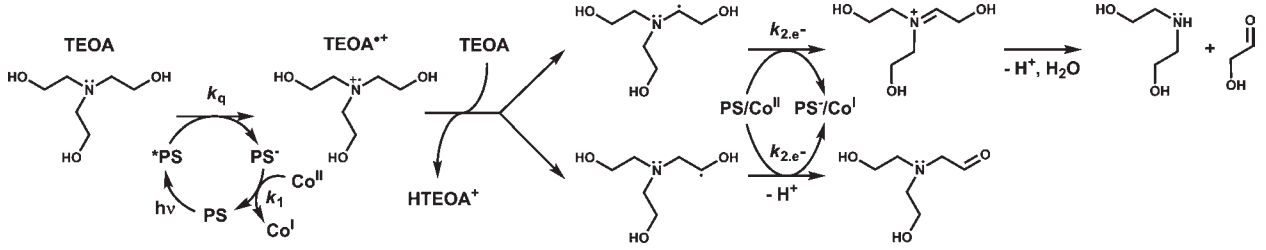

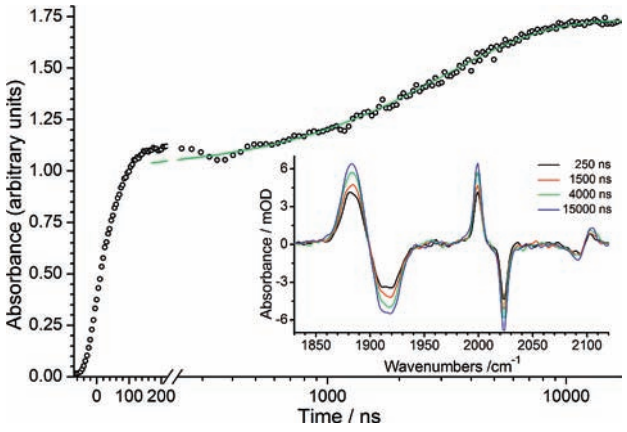

Figure 2. Transient kinetic trace of $\mathbf{1}^-$ (integrated absorbance of CO and NCS bands) in DMF with 1 M TEOA after excitation with $\lambda = 355$ nm (black circles). Oscillation of the signal between ~150 and ~450 ns is caused by amplifier ringing. Green line: Exponential fit of a second rise from 200 ns to 18 μs. Inset: Transient spectra measured at different delay times. Bands pointing downward belong to CO and NCS vibrations of the ground state of **1**, positive bands to those of the reduced complex $\mathbf{1}^-$.

similar to those of $[ReBr(CO)_3bipy]$ (Table 1). As is evident from HPLC analysis, **1** proved to be very inert toward $[NCS]^-$ substitution in DMF. Comparative H_2 formations are given in Figure 1. Further experiments were done to clarify the kinetics in the modified system, namely, the sequence of the catalytic cycle, the influence of the concentration of both $[HTEOA][BF_4]$ and $[Co(dmgH)_2]$, and the long-term performance.

Electron-Transfer Steps. To allow observation of the eventual secondary electron-transfer processes following the first, very fast reduction (k_q; Scheme 2), step-scan IR spectroscopy was applied to cover the time domain from 100 ns to 500 μs. The kinetics of $\mathbf{1}^-$, originating from reductive quenching of ***1** by TEOA (Scheme 2, left side), could thus be analyzed in more detail.[8] The first step after excitation, i.e., quenching of the triplet metal-to-ligand charge-transfer (^{3}MLCT) state of **1**, is not resolved with this method because its time scale is beyond the resolution of the step-scan technique (~11 ns in DMF with [TEOA] = 1 M; Table 1).

A 1 mM solution of **1** with 1 M TEOA in DMF was prepared and purged with Ar for 60 min before irradiation and measurement. Figure 2 shows the kinetic trace of $\mathbf{1}^-$ and difference spectra at various delay times after excitation with 355 nm light. The IR bands at 1918, 2024, and 2092 cm^{-1} correspond to the asymmetric and symmetric CO stretching vibrations and the NCS stretching vibration, respectively. These bands are bleached upon excitation and subsequent reductive quenching of ***1** by TEOA.[8,25] The corresponding ν_{CO} transients of $\mathbf{1}^-$ are found at slightly lower wavenumbers (1884 and 1999 cm^{-1}), indicative of an increased back-bonding in $\mathbf{1}^-$,[8,26,27] while ν_{NCS} of $\mathbf{1}^-$ appears at 2103 cm^{-1}. The kinetic trace of $\mathbf{1}^-$ consists of two processes occurring at different time scales. While the reductive quenching of the ^{3}MLCT state takes place within a few nanoseconds, the signal first rises within the response time of the detector and amplifier, reaching a first plateau after ~200 ns. Subsequently, a second step of the signal with a first-order time constant of 3.1 μs was observed. The amplitude of the second step is ~70% relative to the first one. Reductive quenching of ***1** with TEOA (amplitude: 100%) generates the nitrogen-centered radical-cation $TEOA^{\bullet+}$ $\{N^{\bullet}(CH_2CH_2OH)_3^{+}\}$ (Scheme 2). $H^{\bullet}$ abstraction at TEOA by $TEOA^{\bullet+}$/deprotonation of $TEOA^{\bullet+}$ by TEOA yields the carbon-centered radicals $(HOCH_2C^{\bullet}H)N(CH_2CH_2OH)_2$ and/or $(HOC^{\bullet}HCH_2)N(CH_2CH_2OH)_2$, as shown before (Scheme 2, right side).[28−34] Unlike the aminyl radical $TEOA^{\bullet+}$, these carbon-centered radicals are strong reducing agents[28,32]

(25) Rodriguez, A. M. B.; Gabrielsson, A.; Motevalli, M.; Matousek, P.; Towrie, M.; Sebera, J.; Zalis, S.; Vlcek, A. *J. Phys. Chem. A* **2005**, *109*, 5016–5025.
(26) George, M. W.; Johnson, F. P. A.; Westwell, J. R.; Hodges, P. M.; Turner, J. J. *J. Chem. Soc., Dalton Trans.* **1993**, 2977–2979.
(27) Hayashi, Y.; Kita, S.; Brunschwig, B. S.; Fujita, E. *J. Am. Chem. Soc.* **2003**, *125*, 11976–11987.
(28) Chan, S. F.; Chou, M.; Creutz, C.; Matsubara, T.; Sutin, N. *J. Am. Chem. Soc.* **1981**, *103*, 369–379.
(29) Delaive, P. J.; Foreman, T. K.; Giannotti, C.; Whitten, D. G. *J. Am. Chem. Soc.* **1980**, *102*, 5627–5631.
(30) Kalyanasundaram, K. *J. Chem. Soc., Faraday Trans.* **1986**, *82*, 2401–2415.
(31) Neshvad, G.; Hoffman, M. Z. *J. Phys. Chem.* **1989**, *93*, 2445–2452.
(32) Kishore, K.; Dey, G. R.; Mukherjee, T. *Res. Chem. Intermed.* **2004**, *30*, 837–845.
(33) Kirch, M.; Lehn, J. M.; Sauvage, J. P. *Helv. Chim. Acta* **1979**, *62*, 1345–1384.
(34) Kalyanasundaram, K.; Kiwi, J.; Gratzel, M. *Helv. Chim. Acta* **1978**, *61*, 2720–2730.

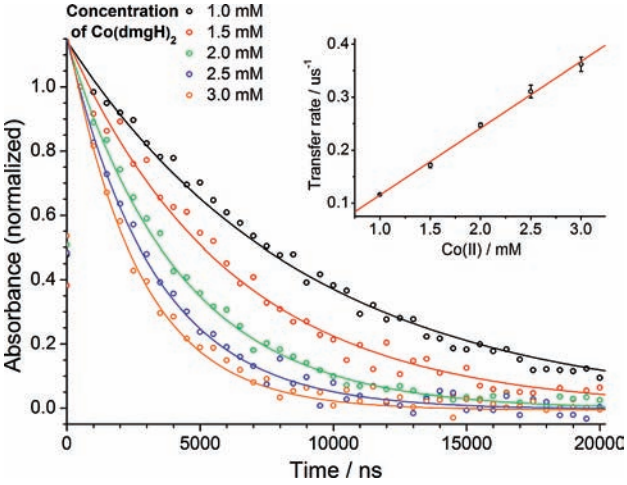

Figure 3. Transient kinetic traces for $\mathbf{1}^-$ (integrated absorbance of CO and NCS bands) in the presence of different concentrations of [Co(dmgH)$_2$] after excitation with λ = 355 nm. Inset: Time constants of the decay of $\mathbf{1}^-$ as a function of the concentration of [Co(dmgH)$_2$]. Linear fitting gives the rate for the forward electron-transfer reaction ($\mathbf{1}^-$ + [Co^{II}(dmgH)$_2$] → **1** + [Co^{I}(dmgH)$_2$]$^-$).[38]

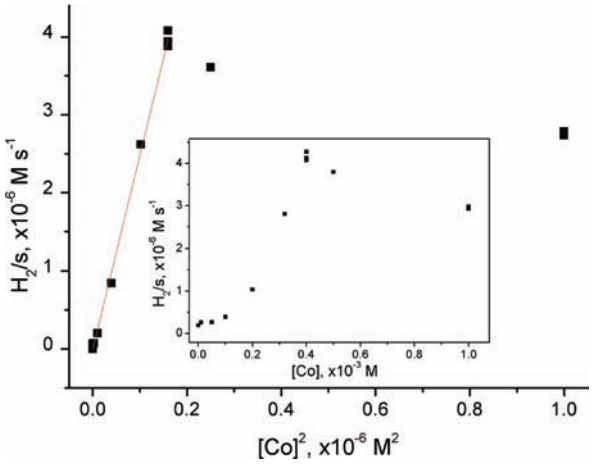

Figure 4. Initial H_2 production rates as a function of [Co]^2. Inset: Initial H_2 production rates as a function of [Co]; 0.5 mM **1**, varying {[Co(OH$_2$)$_6$](BF$_4$)$_2$, 6 dmgH$_2$}, 1 M TEOA, 0.1 M HBF$_4$, DMF, Ar, 476 nm.

that prevent back electron transfer from $\mathbf{1}^-$. In addition, they donate a second electron[28−31,33,35,36] to **1** with a yield of ∼70%, rationalizing the kinetic trace depicted in Figure 2. An upper limit of ∼40 μM for $\mathbf{1}^-$ and, therefore, for (HOCH$_2$C$^{\bullet}$H)N(CH$_2$CH$_2$OH)$_2$ and/or (HOC$^{\bullet}$HCH$_2$)-N(CH$_2$CH$_2$OH)$_2$ after reductive quenching was calculated from the spectral overlap of **1** and the laser pulse (355 nm and 2 mJ). Thus, after transfer of the second electron, the concentration of $\mathbf{1}^-$ is ∼70 μM. Because of the large excess of **1**, its concentration can be considered to be constant. The resulting pseudo-first-order kinetics for transfer of the second electron gives a rate constant of $k_{2e^-} = 3.3 \times 10^8$ M^{-1} s^{-1}. The yield of less than 100% might result from other deactivation pathways such as recombination or disproportionation, which radicals typically undergo.

In order to quantify the electron-transfer rates in this new system, we kept all components constant (1 mM **1**, 1 M TEOA, and 0.1 M HBF$_4$) but varied Co^{II} from 1.0 to 3.0 mM in 0.5 mM steps. [Co(OH$_2$)$_6$](BF$_4$)$_2$ was dissolved with a 6-fold excess of dmgH$_2$ to ensure the complete formation of [Co^{II}(dmgH)$_2$]. Transient kinetic traces of $\mathbf{1}^-$ are shown in Figure 3. $\mathbf{1}^-$ transfers its electron to [Co^{II}(dmgH)$_2$], thereby generating a Co^{I} species. Because of a large excess, the Co^{II} concentration remains almost constant, which results in pseudo-first-order kinetics for the decay of $\mathbf{1}^-$. An exponential fit gave the following lifetimes with increasing concentrations of Co^{II}: 8.9, 6.1, 4.2, 3.3, and 2.7 μs. The corresponding rates depend linearly on the Co^{II} concentration, thus giving $k_1 = 1.3 \times 10^8$ M^{-1} s^{-1} for the electron-transfer step (Figure 3). This rate is in good agreement with a similar report in the literature[2] and compares well with electron transfer between [ReBr(CO)$_3$bipy]$^-$ and [Co^{II}(dmgH$_2$)] ($k_{1,Br} = 2.5 \times 10^8$ M^{-1} s^{-1}).[8] From Table 1 and E(Co$^{II/I}$) = −1.040 V, the corresponding backward electron-transfer rate is estimated as $k_{-1} \approx 4.1 \times 10^5$ M^{-1} s^{-1} ($\Delta_R G$ = −14.3 kJ mol^{-1}) and $k_{-1,Br} \approx 1.1 \times 10^5$ M^{-1} s^{-1} ($\Delta_R G$ = −19.1 kJ mol^{-1}) for **1** and [ReBr(CO)$_3$bipy], respectively, as was expected for an electron transfer in the normal region according to the Marcus theory. As found for similar systems (PS = ruthenium, platinum, or iridium complex; WRC = cobalt or rhodium complex),[6,9,37] quenching of ***1** by cobalt occurs at a rate close to diffusion control (see SI 8 in the Supporting Information; $k_d = 5 \times 10^9$ M^{-1} s^{-1} in 1 M TEOA, DMF).[8,36] Because $k_{q,TEOA} = 9.2 \times 10^7$ M^{-1} s^{-1} and [TEOA] = 1 M in all of our experiments, negligible contribution from quenching by cobalt is expected.

Cobalt Dependence. By systematically varying the cobalt concentrations, we showed that H_2 evolution in the original [ReBr(bipy)(CO)$_3$]/acetic acid system occurred along a second-order process in cobalt with $k_{obs} = 4$ M^{-1} s^{-1}.[8] In the new and improved system, a linear fitting of dH_2/dt vs [Co]$_{tot}$ gave $k_{obs} = 25$ M^{-1} s^{-1} (Figure 4).

The second-order process was rationalized by a bimolecular reaction of two cobalt hydrides as the rate-limiting elementary step (eqs 1−3), as postulated elsewhere.[39,40] Assuming a fast preequilibrium for eq 2 and with substitution of [Co^{I}] for c[Co]$_{tot}$, where c is the fraction of Co^{I} with respect to [Co]$_{tot}$, eq 4 describes the relationship

(35) Kutal, C.; Corbin, A. J.; Ferraudi, G. *Organometallics* **1987**, *6*, 553–557.
(36) Kutal, C.; Weber, M. A.; Ferraudi, G.; Geiger, D. *Organometallics* **1985**, *4*, 2161–2166.
(37) Krishnan, C. V.; Brunschwig, B. S.; Creutz, C.; Sutin, N. *J. Am. Chem. Soc.* **1985**, *107*, 2005–2015.
(38) It should be noted that the treatment of the transients as simple exponential decays ignores a possible influence of the second electron being transferred from the oxidized form of TEOA. In fact, this contribution is detectable for small concentrations of Co^{II} (i.e., < 1 mM), while it is negligible for larger ones, as is obvious from Figure 3. It is therefore reasonable to consider also a direct electron transfer from (HOCH$_2$C$^{\bullet}$H)-N(CH$_2$CH$_2$OH)$_2$ and/or (HOC$^{\bullet}$HCH$_2$)N(CH$_2$CH$_2$OH)$_2$ to [Co^{II}(dmgH)$_2$] in addition to the transfer to **1**. The former route becomes dominant for higher concentrations of [Co^{II}(dmgH)$_2$]. The direct transfer does not alter the kinetic trace of $\mathbf{1}^-$, provided that [Co^{II}] remains approximately constant.
(39) Dempsey, J. L.; Winkler, J. R.; Gray, H. B. *J. Am. Chem. Soc.* **2010**, *132*, 1060–1065.
(40) Hu, X.; Brunschwig, B. S.; Peters, J. C. *J. Am. Chem. Soc.* **2007**, *129*, 8988–8998.

Scheme 3. Schematic Representation of the Proposed Reaction Cycles to H_2

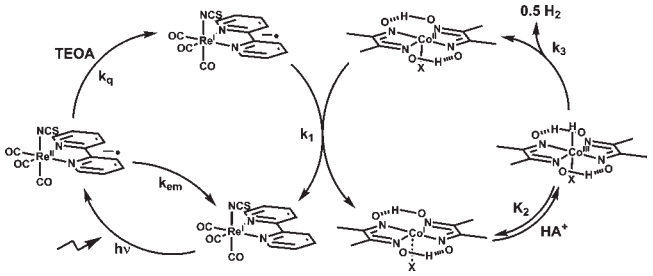

between the rate of H_2 formation and the total cobalt concentration.

$$Co^{II} + \mathbf{1}^- \rightarrow Co^{I} \quad (k_1) \tag{1}$$

$$Co^{I} + HA^+ \rightarrow Co^{III}\text{-}H + A \quad (K_2) \tag{2}$$

$$2Co^{III}\text{-}H \rightarrow 2Co^{II} + H_2 \quad (k_3) \tag{3}$$

$$\frac{dH_2}{dt} = k_3 K_2{}^2 \left(\frac{[HA^+]}{[A]}\right)^2 c^2 [Co]_{tot}{}^2 = k_{obs}[Co]_{tot}{}^2 \tag{4}$$

A systematic variation of $[HA^+]/[A]$ would allow one to identify $k_3K_2{}^2c^2$. This experiment is hardly possible with acetic acid because it is not clear if AcOH or internally generated $[HTEOA]^+$ did serve as the proton source. In the present study, $[HA^+]/[A]$ was fixed at 0.11 and $k_3K_2{}^2c^2$ thus equals 2025 M^{-1} s^{-1}.

We observed a very poor long-term performance when cobalt became rate-limiting ([Co] < 0.4 mM). When the reaction was run to completion under these conditions (H_2 evolution ceased), a black precipitate formed, the solution became colorless, and **1** could no longer be detected by HPLC. When cobalt becomes rate-limiting, complex $\mathbf{1}^-$, a strong reductant (−1.185 V vs Ag/AgCl) with a lifetime well above 10 ms as determined by transient IR spectroscopy in DMF/TEOA solutions, accumulates in the solution (Scheme 3). While being sufficiently long-lived to react with Co^{II} (≈16 μs for $[Co^{II}] = 0.5$ mM with $k_1 = 1.3 \times 10^8$ M^{-1} s^{-1}), this radical has a chemistry of its own. In the complete absence of cobalt but with $[HTEOA]^+$, 3−5 equiv of H_2 and a black precipitate were observed (end $TON_{Re} = 4 \pm 1$), revealing a competitive, destructive pathway ending the catalytic cycle.

Acid Dependence. Replacement of acetic acid by $[HTEOA][BF_4]$ substantially improved the long-term performance. There are several reasons why acetic acid affects H_2 production, namely, its interaction with the PS (see before), but also its high pK_a in DMF ($pK_{a,AcOH}$ = 13−14; $pK_{a,TEOA}$ = 7.5; both in DMF),[23] making it a less likely proton source in eq 2. To quantify the role of $[HTEOA][BF_4]$, its concentration was varied systematically from 0 to 0.2 M, while all other parameters were kept constant (Figure 5). A distinct dependence was found for the initial TOFs, reaching a plateau at $[HBF_4] \geq 0.1$ M,

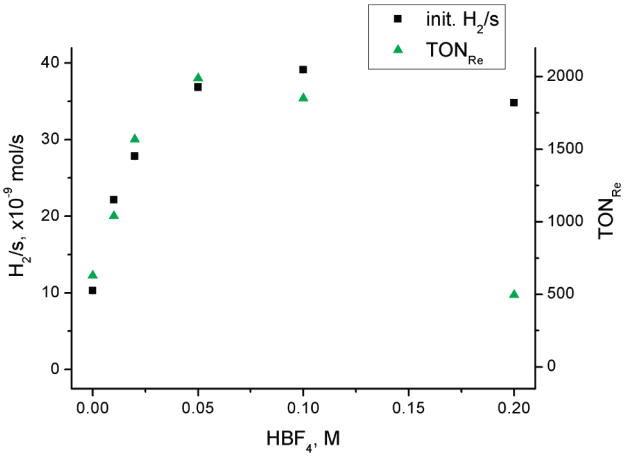

Figure 5. Left scale: initial H_2 production rates. Right scale: total TON_{Re} as a function of $[HBF_4]$ (0.5 mM **1**, 0.5 mM $[Co(OH_2)_6](BF_4)_2$, 3 mM $dmgH_2$, 1 M TEOA, DMF, Ar, 476 nm).

Table 2. HPLC Analysis of Free $dmgH_2$ and **1** during Catalysis (See Also SI 2 in the Supporting Information)[a]

irradiation time, h	$dmgH_2$, %	**1**, %	TOF_{Re}, H/Re/h	TON_{Re}, H/Re
0	100	100	56	0
16	80	100	32	670
55	0	80	10	1380
120	0	0	0	1850

[a] 1 M TEOA, 0.1 M HBF_4, 0.5 mM **1**, 0.5 mM {$[Co(OH_2)_6](BF_4)_2$, 6 $dmgH_2$}, DMF, Ar, 476 nm.

indicating rate-limiting protonation of $[Co^I]$ (eq 2) for $[HBF_4] \leq 0.1$ M. Slow H_2 formation was observed even in the absence of acid. Obviously, HBF_4 is not the sole proton source because the photocatalytic oxidation of TEOA generates two protons, compensating for the formal H^+ loss by H_2 formation (see Scheme 2).[30,41] In fact, for most experiments, more H_2 was produced than protons added in the form of HBF_4, thus underscoring the importance of proton release upon decomposition of $TEOA^{\bullet+}$ (Scheme 2, right side).

Besides the acid-dependent TOFs, the acid concentration had a marked influence on the final TON_{Re}. At $[HBF_4] = 0.2$ M, the initial TOF (TOF_{ini}) compares well with the fastest one at 0.1 M, but the final TON_{Re} was only ≈25% of the maximum TON at 50 mM HBF_4 (2000 H/Re). At low $[HBF_4]$, the final TON_{Re} correlated well with TOF_{ini}. Analyzing the solutions after H_2 formation ceased, we found that $dmgH_2$ and **1** disappeared. A continuous analysis of the reaction with 0.1 M HBF_4 first revealed the disappearance of $dmgH_2$, followed by subsequent decomposition of **1** (Table 2).

The time-dependent concentrations, as shown in Table 2, imply a slow decomposition of the cobalt catalyst as the primary reason for the decay of the TOF over time. This deactivation pathway occurs slowly and is indirectly evidenced by the consumption of free $dmgH_2$. The fact that H_2 production ceased quite abruptly after 120 h is also in support of this interpretation (see SI 2 in the Supporting Information). To corroborate this hypothesis, we quantified the TON as a function of the $dmgH_2$ concentration (see SI 3 in the Supporting Information).

(41) Sun, H.; Hoffman, M. Z. *J. Phys. Chem.* **1994**, *98*, 11719–11726.

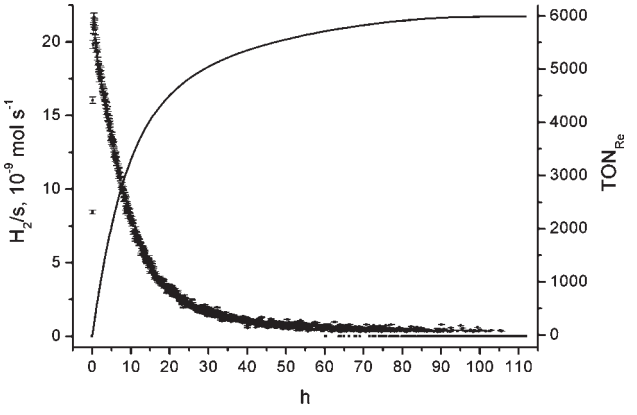

Figure 6. H_2 production rate (left scale, ■) and TON_{Re} (right scale, black line) as a function of time (30 μM **1**, 0.5 mM $[Co(OH_2)_6](BF_4)_2$, 3 mM $dmgH_2$, 1 M TEOA, 20 mM HBF_4, DMF, Ar, 380 nm).

The addition of more than 4−6 equiv of $dmgH_2$ did not significantly change the rate of H_2 formation. However, TON_{Re} increased steadily with increasing [$dmgH_2$], supporting $dmgH_2$ consumption to be the TON-limiting process. It was postulated before that [Co^{III}-H], in a slow reaction, undergoes intramolecular hydride shift to the coordinated oxime moiety of dmgH to give a hydroxylamine derivative.[42]

Long-Term Performance. Long-term stability with the new system is among the best reported so far (TON_{Re} up to 2000), but catalysis still slowed down over time. In these long-term experiments, a substantial part of TEOA was sacrificed (up to 50% for 2 electrons per TEOA). According to our analyses, decomposition of $[Co(dmgH)_2]$ dominates the rate decrease and long-term stability. Depletion of TEOA, as a substrate in the process, contributes to the activity loss but not to the long-term performance because the addition of TEOA up to the original concentration at a late time point did not increase TOF or final TONs. Consequently, when the concentration of **1** was decreased to 30 μM and upon irradiation with a 380 nm high-flux LED, TON_{Re}'s up to 6000 were observed (Figure 6 and SI 4 in the Supporting Information) while less than 10% TEOA (for 2 electrons) was consumed. These high TON_{Re}'s can only be achieved if decomposition of **1** is not limiting. The fact that TON_{Co} (H_2 per cobalt) never exceeded ~1000 (~200 per $dmgH_2$) was a further strong indication for decomposition of $[Co(dmgH)_2]$ to be the responsible factor for performance limitation.

Dependence on Photon Flux, Quantum Yield, and Colloids. The rates of H_2 formation depended linearly on the photon flux as determined by actinometry (see SI 5 in the Supporting Information). Quantification of the quantum yields should be addressed with care because of two systematic uncertainties, namely, the second electron released upon oxidation of TEOA and absorption of the reduced cobalt catalyst. The former uncertainty potentially gives an upper limit of $\Phi_{H/h\nu} = 200\%$, whereas the latter alters the observed $\Phi_{H/h\nu}$ as a function of the wavelength and can only be eliminated if the concentration and extinction of the reduced cobalt catalyst are known. The observed quantum yield for a standard experiment (0.5 mM **1**, 0.5 mM $[Co(OH_2)_6](BF_4)_2$, 3 mM $dmgH_2$, 1 M TEOA, 0.1 M HBF_4, DMF, Ar, 380 nm) was found to be $\Phi_{H/h\nu,380nm} \approx 90\%$ (observed H/absorbed photon), as compared to $\Phi_{H/h\nu,380nm} \approx 40\%$ (observed H/absorbed photon) for the original $[ReBr(CO)_3bipy]$/acetic acid system (0.5 mM $[ReBr(CO)_3bipy]$, 1 mM $[Co(ac)_2(H_2O)_4]$, 6 mM $dmgH_2$, 1 M TEOA, 0.1 M AcOH, DMF, Ar, 380 nm). We previously reported an observed quantum yield of 26%, which was obtained in a different setup at 415 nm, thus at different optical densities in cobalt.[8] If the yield of the second electron released by $(HOCH_2C^{\bullet}H)N(CH_2CH_2OH)_2$ and/or $(HOC^{\bullet}HCH_2)$-$N(CH_2CH_2OH)_2$ (see the section Electron-Transfer Steps) is taken into account, the quantum yield reduces to 90%/1.7 ≈ 50%.

To exclude colloids as catalytically active species, as established for similar systems with noble metal WRC catalysts,[11−14,43] it was of special interest to assess a homogeneous reaction in the present system. Evidence for homogeneous H_2 formation with $[Co(dmgH)_2]$ was already received from light scattering,[8] from mercury poisoning experiments,[6] and, indirectly, from electrochemical studies.[40,44] The squared dependence of H_2 formation in $[Co]_{tot}$ as reported herein is not expected for a heterogeneous system. Because Hg^0 is known to poison colloidal catalysts, qualitative poisoning studies as reported in the literature for other systems were performed.[9,45,46] If a colloidal species would be the source of H_2 formation, the addition of elemental mercury would affect the long-term performance. In a test experiment, two solutions (0.5 mM **1**, 0.5 mM $[Co(OH_2)_6](BF_4)_2$, 3 mM $dmgH_2$, 1 M TEOA, 0.1 M HBF_4, DMF, Ar, 476 nm) were irradiated for 13.5 h with or without Hg^0 (200 μL and 2500 equiv relative to rhenium and cobalt, respsectively). Mercury was then removed and the experiment continued (see SI 6 in the Supporting Information). The shapes of the curves [H_2]/s vs time were identical, with or without mercury, being in agreement with a homogeneous process.[47]

Conclusion

Photocatalytic systems for H_2 formation based on $[ReX(bipy)(CO)_3]$ as the PS and $[Co(dmgH)_2]$ as the H_2 evolution reaction catalyst are alternatives to the widely studied ruthenium systems. Identifying the deactivation pathways in such a system is key for the development of long-term stable systems. The loss of the axial Br^- ligand in the PS is one of these pathways. Exchanging Br^- with $[NCS]^-$

(42) Simandi, L. I.; Szeverenyi, Z.; Budozahonyi, E. *Inorg. Nucl. Chem. Lett.* **1975**, *11*, 773–777.

(43) Du, P.; Schneider, J.; Fan, L.; Zhao, W.; Patel, U.; Castellano, F. N.; Eisenberg, R. *J. Am. Chem. Soc.* **2008**, *130*, 5056–.

(44) Razavet, M.; Artero, V.; Fontecave, M. *Inorg. Chem.* **2005**, *44*, 4786–4795.

(45) Paklepa, P.; Woroniecki, J.; Wrona, P. K. *J. Electroanal. Chem.* **2001**, *498*, 181–191.

(46) Anton, D. R.; Crabtree, R. H. *Organometallics* **1983**, *2*, 855–859.

(47) Because our reaction flasks were irradiated with an LED from below, effective photon flux in the mercury experiment was lower than that without mercury (reflected in the lower TOF but identical shape of the curve in SI 6 in the Supporting Information). If mercury would poison our catalysts, one would par contra expect that catalysis would not take place at all or come to a stop shortly after the start. To further confirm the hypothesis about the reduced photon flux, mercury was removed after 13.5 h and the experiment continued. H_2 production now indeed proceeds at rates identical with those in an experiment in which no mercury was added in the first place.

and replacing AcOH by $[HTEOA]^+$ with noncoordinating $[BF_4]^-$ as the counterion increased the efficiency considerably in terms of both the quantum yield and final TON, thus underlining the crucial importance of X^-. With the new and very stable PS [Re(NCS)(bipy)$(CO)_3$], the stability of [Co$(dmgH)_2$] became performance-limiting, most likely because of an intramolecular hydride shift of [Co^{III}-H] to a coordinated oxime moiety. To further improve this system requires thus stabilization of the cobalt complex toward hydride shift or an increase in the rate of H_2 formation with respect to the hydride shift, while keeping further physicochemical parameters intact. Detailed studies about the decomposition pathways of the cobalt complex are underway.

Experimental Section

All chemicals were of reagent grade and were used without further purification. Spectroscopic-grade DMF, $Co(BF_4)_2 \cdot 6H_2O$, and coumarin I were purchased from Acros. Electrochemical-grade [TBA](PF_6), [TBA]Br, TEOA, $[Et_2OH](BF_4)$, $[Co(ac)_2(H_2O)_4]$, $dmgH_2$, phenanthroline, and ethanol were purchased from Fluka. Water was doubly distilled before use. Synthetic reactions were carried out under N_2 or Ar using standard Schlenk techniques. HBF_4 in the text refers to [HTEOA](BF_4), synthesized from TEOA and $[Et_2OH](BF_4)$.[48] The syntheses of **1**, [ReBr$(CO)_3$bipy], [Re$(OH_2)(CO)_3$bipy](TflsO), [Co$(dmgH)_2$], and $K_3[Fe(ox)_3]$ have been described in the literature.[8,24]

Luminescence measurements were performed on a Perkin-Elmer LS50B fluorescence spectrometer with Ar-purged solution samples in 1 cm cells. Luminescence lifetime measurements were performed on an Edinburgh Instrument F900 equipped with an F900 ns flash lamp filled with H_2 (operating at 0.4 bar and a frequency of 40 kHz). Luminescence quantum yields were determined relative to coumarin I in ethanol (0.64)[49] according to a literature procedure.[50]

UV−vis spectra were measured using a Cary 50 spectrometer with solution samples in 1 cm quartz cells. If necessary, cells with silicon septa lids were used to keep samples under an inert-gas atmosphere during measurements.

IR spectra were recorded on a Bio-Rad FTS-45 spectrometer with samples in compressed KBr pellets.

Electrochemical measurements were carried out in DMF containing 0.1 M [TBA][PF_6] as the conducting electrolyte. A Metrohm 757VA Computrace electrochemical analyzer was used with a standard three-electrode setup of glassy carbon working (i.d. = 3 mm) and platinum auxiliary electrodes and an Ag/AgCl reference electrode. All potentials are given vs Ag/AgCl and are referenced with Fc/Fc^+ at +500 mV.

HPLC measurements were performed on a VWR LaChrome Elite using a Nucleodur C18 gravity column operated in an oven (L-2350) at 40 °C and a PDA detector (L-2450). The gradient was as follows: A = 0.1% TFA, 10% MeOH, and H_2O; D = MeOH; flow rate = 0.5 mL min^{-1}; 0−5 min, 100% A; 5−15 min, 0−100% D; 15−18 min, 100% D. Control runs before and after catalysis were systematically performed using 10 μL of the reaction solution in DMF. Under these conditions, $dmgH_2$ gave a broad peak at 6.4 min and **1** a defined peak at 17.04 min.

Gas chromatograms were recorded using a Varian CP-3800 gas chromatograph with Ar as the carrier gas and a 3 m × 2 mm packed molecular sieve 13X 80-100 column. The gas flow was set to 20 mL min^{-1}. The oven was operated isothermally at 100 °C. An Ar flow of usually 21.6 mL min^{-1} [adjusted with a manual flow controller (Porter, 100) and referenced with a flowmeter (MS Wil GmbH)] was passed through the reaction mixture and into the gas chromatograph, where 100 μL gas samples were automatically injected in defined time intervals (usually 5 min) using a 6-port−2-position valve from Vicci. The gases were detected using a thermal conductivity detector (Varian) operated at 150 °C. H_2 production rates were calibrated by introducing a known flow of pure H_2 by a single syringe pump (70-2208 from Harvard Apparatus, using a 2.5 mL Hamilton GASTIGHT #1002 syringe and a Teflon tube) to the 60 mL Schlenk containing 1 M TEOA in DMF. Plotting of the peak area for H_2 versus the used flow rates of H_2 gave linear fits. The slopes of these fits depended linearly on the Ar flow through the solution. Varying the Ar flow thus allowed the detection of smaller H_2 production rates, although at a higher response time (10 min for 21.6 mL min^{-1}).

Photochemical measurements were carried out in a 60 mL septum-capped Schlenk tube containing a Teflon stirrer at 500 rpm. A total of 10 mL of a solution containing the respective mixture in DMF was prepared, wrapped in black foil, and degassed using an Ar-purged Schlenk line. The mixture was equilibrated under 1.5 bar of Ar pressure for 15 min and then transferred to a dark room for illumination. The light source was either a 380 or 476 nm high-flux LED from Rhopoint Components Ltd. (OTLH-0280-UV or OTLH-0010-BU, respectively; CPC reflector for Shark LED; irradiated directly from below; current control at usually 200 mA; $h\nu/s = 1.75 \times 10^{-7}$ and 2×10^{-7} mol s^{-1}, respectively). If necessary, the radiant flux was varied by adjustment of the current through the LED. The radiant flux at different currents was calibrated using actinometry. A constant flow of usually 21.6 mL min^{-1} of Ar was passed through the solution and into a six-port valve at the gas chromatograph, where 100 μL gas samples were injected into the gas chromatography/thermal conductivity detector (GC/TCD) gas analyzer in defined intervals. Integration of the production rate versus time gave the total amount of H_2 produced.

Quantum yields were determined in a 1 cm quartz cell using a 380 nm LED (OTLH-0280-UV, Rhopoint Components Ltd.) in series with an iris and a lens to ensure linear photon flux. The cells were filled with 2 mL solutions as follows: 0.5 mM **1** ($1 - T = 0.957 \pm 0.0033$) and [ReBr$(CO)_3$bipy] ($1 - T = 0.971 \pm 0.0028$), 0.5 mM {$[Co(OH_2)_6](BF_4)_2$, 6 $dmgH_2$} and 1 mM {$Co(ac)_2(H_2O)_4$], 6 $dmgH_2$}, 1 M TEOA, and 0.1 M HBF_4 for AcOH, DMF, and Ar, respectively. The total H_2 was determined by manual sampling of 20 μL of head-space gas through a septum and subsequent injection into a GC/TCD system as described above. The photon flux as determined by actinometry was $4.81 \pm 0.13 \times 10^{-9}$ mol s^{-1}. It was corrected for the respective fractions of light absorbed. The H_2 production rates measured were $(2.18 \pm 0.082) \times 10^{-9}$ and $(1.01 \pm 0.069) \times 10^{-9}$ mol s^{-1} for **1** and [ReBr$(CO)_3$bipy], respectively.

Actinometry for the quantum yield determination was performed in a 1 cm quartz cell containing 2 mL of 9 mM $K_3[Fe(ox)_3]$ in 0.1 N H_2SO_4 as the chemical actinometer and was irradiated as described in quantum yields ($1 - T$ for $K_3[Fe(ox)_3] > 0.999$). For calibration of the photon flux in the standard setup, a setup identical with that for H_2 production (LED from below, varying current, 60 mL Schlenk, stirred, Ar flow of 21.6 mL min^{-1}) was used with 10 mL of a 9 mM $K_3[Fe(ox)_3]$ in 0.1 N H_2SO_4 as the chemical actinometer. Analysis of irradiated solutions: after a certain time at a certain LED current, 100 μL of the irradiated solution was added to 100 μL of a 5 mM solution of phenanthroline in H_2O, agitated, and left in the dark for 30 min. After this, 50 μL of a 600 mM NaOAc/360 mN H_2SO_4 buffer and 750 μL

(48) Ono, H.; Seki, R.; Ikeda, R.; Ishida, H. *J. Mol. Struct.* **1995**, *345*, 235–243.
(49) Olmsted, J. *J. Phys. Chem.* **1979**, *83*, 2581–2584.
(50) Williams, A. T. R.; Winfield, S. A.; Miller, J. N. *Analyst* **1983**, *108*, 1067–1071.

of H_2O were added and absorption at 511 nm was determined relative to a solution that was not irradiated. Conversion to photon flux as a function of the LED current was achieved by using $\varepsilon_{[Fe^{II}(phen)_3],511nm} = 10750 \pm 76\ M^{-1}\ cm^{-1}$ and $\eta_{Fe^{III} \rightarrow Fe^{II}} = 1.18$ and 0.925 for 380 and 476 nm, respectively.[51]

Time Resolved Step-Scan FTIR Spectroscopy. The kinetics of the electron transfer from reductively quenched $\mathbf{1}^-$ to cobalt were measured through time-resolved step-scan IR spectroscopy. The system consists of a FT-IR spectrometer (Bruker Vertex 80 V) equipped with a PV mercury−cadmium−telluride detector and a frequency-tripled Nd:YAG laser generating pulses of ~2 mJ per < 10 ns at 355 nm with a repetition rate of 10 Hz used for sample excitation. The nominal time resolution that is reached with this setup is about 100 ns. The sample was continuously pumped through a 200 μm cell with 19.5 mL min^{-1}, giving an exchange rate for the probe volume of 14.5 s^{-1} in our case. A small sealed reservoir ($V \approx 3$ mL) was included between the peristaltic pump and the sample cell to minimize pulsation inside the latter. To avoid any interference of the pumping system with the aggressive sample mixture, a calcium fluoride sample cell with Teflon tubing was used. For sealings and the peristaltic pump tubing, chemically resistant perfluoroelastomers (ChemSure) were chosen. The samples were prepared by mixing all components except for $[Co(OH_2)_6](BF_4)_2$ in the form of standardized solutions in DMF, followed by filtration through a Teflon syringe filter (0.2 μm pore size). The solution was then purged for 30 min, after which $Co(BF_4)_2$ was added as a degassed solution in DMF. The measurements were started after an additional 30 min of purging, while the sample was already pumped through the flow cell. After the measurements, all samples were checked via static IR spectroscopy, entirely showing negligibly small degradation caused by irradiation at 355 nm.

(51) Hatchard, C. G.; Parker, C. A. *Proc. R. Soc. London A* **1956**, *235*, 518–536.

Acknowledgment. We are grateful to the Swiss National Science Foundation for financially supporting this work (Grant 200021-119798).

Supporting Information Available: H_2 formation as a function of the bromide concentration, in a typical experiment, as a function of the [Co]/[$dmgH_2$] ratio, at low [**1**], and as a function of photon flux, with added mercury and quenching rates of ***1** by different cobalt complexes. This material is available free of charge via the Internet at http://pubs.acs.org.